Article

Density Functional Theory Study on a Missing Piece in Understanding of Heme Chemistry: The Reaction Mechanism for Indoleamine 2,3-Dioxygenase and Tryptophan 2,3-Dioxygenase

Lung Wa Chung, Xin Li, Hiroshi Sugimoto, Yoshitsugu Shiro, and Keiji Morokuma

J. Am. Chem. Soc., **2008**, 130 (37), 12299-12309 • DOI: 10.1021/ja803107w • Publication Date (Web): 20 August 2008

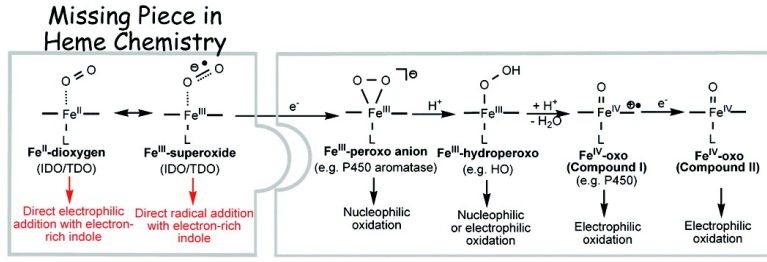

More About This Article

Additional resources and features associated with this article are available within the HTML version:

- Supporting Information
- Access to high resolution figures
- Links to articles and content related to this article
- Copyright permission to reproduce figures and/or text from this article

View the Full Text HTML

J|A|C|S
ARTICLES

Published on Web 08/20/2008

Density Functional Theory Study on a Missing Piece in Understanding of Heme Chemistry: The Reaction Mechanism for Indoleamine 2,3-Dioxygenase and Tryptophan 2,3-Dioxygenase

Lung Wa Chung,[†] Xin Li,[†] Hiroshi Sugimoto,[‡] Yoshitsugu Shiro,[‡] and Keiji Morokuma*,[†]

Fukui Institute for Fundamental Chemistry, Kyoto University, Kyoto 606-8103, Japan, and Biometal Science Laboratory, RIKEN SPring-8 Center, Harima Institute, Hyogo 679-5148, Japan

Received April 27, 2008; E-mail: morokuma@fukui.kyoto-u.ac.jp

Abstract: Indoleamine 2,3-dioxygenase (IDO) and tryptophan 2,3-dioxygenase (TDO) are heme-containing dioxygenases and catalyze oxidative cleavage of the pyrrole ring of L-tryptophan. On the basis of three recent crystal structures of these heme-containing dioxygenases, two new mechanistic pathways were proposed by several groups. Both pathways start with electrophilic addition of the Fe(II)-bound dioxygen concerted with proton transfer (oxygen ene-type reaction), followed by either formation of a dioxetane intermediate or Criegee-type rearrangement. However, density functional theory (DFT) calculations do not support the proposed concerted oxygen ene-type and Criegee-type rearrangement pathways. On the basis of DFT calculations, we propose a new mechanism for dioxygen activation in these heme systems. The mechanism involves (a) direct electrophilic addition of the Fe(II)-bound oxygen to the C2 or C3 position of the indole in a closed-shell singlet state or (b) direct radical addition of the Fe(III)−superoxide to the C2 position of the indole in a triplet (or open-shell singlet) state. Then, a radical-recombination or nearly barrierless charge-recombination step from the resultant diradical or zwitterionic intermediates, respectively, proceeds to afford metastable dioxetane intermediates, followed by ring-opening of the dioxetanes. Alternatively, homolytic O−O bond cleavage from the diradical intermediate followed by oxo attack and facile C2−C3 bond cleavage could compete with the dioxetane formation pathway. Effects of ionization of the imidazole and negatively charged oxyporphyrin complex on the key dioxygen activation process are also studied.

1. Introduction

Indoleamine 2,3-dioxygenase (IDO) and tryptophan 2,3-dioxygenase (TDO) cleave the pyrrole ring of L-tryptophan (L-Trp) and insert both oxygen atoms of a dioxygen molecule into the organic substrate to afford *N*-formylkynurenine **VI** (Scheme 1).[1,2] This oxidative cleavage of Trp is the first and rate-limiting step in L-Trp catabolism through the kynurenine pathway.[3] IDO is a monomeric enzyme and has broader substrate specificity than TDO. Other indoleamines including D-tryptophan, D- and L-5-hydroxytryptophan, serotonin, and tryptamine are also active substrates of IDO.[4] In addition, IDO is found to be ubiquitously distributed in mammals except the liver. On the other hand, TDO is a homotetrameric enzyme and displays high substrate specificity.[1e] TDO is found in the bacteria or the liver of the mammals. The importance of IDO and TDO is associated with a few important physiological roles, such as suppression of T-cell proliferation, the synthesis of the neuron-transmitter serotonin, and the hormone melatonin.[1e,5]

In sharp contrast with heme-containing monooxygenases (such as cytochrome P450, peroxidase, and heme oxygenase) and nonheme dioxygenases (catechol dioxygenases and naphthalene dioxygenase),[1e,6] the reaction mechanism for this oxidation in IDO and TDO remains elusive, even thought they were discovered more than 40 years ago.[1] It is mainly due to the lack of structural determinations for IDO or TDO containing heme and observation of the proposed intermediates, as well

[†] Kyoto University.
[‡] RIKEN SPring-8 Center.

(1) (a) Kotake, Y.; Masayama, I. *Z. Physiol. Chem.* **1936**, *243*, 237. (b) Hayaishi, O.; Rothberg, S.; Mehler, A. H.; Saito, Y. *J. Biol. Chem.* **1957**, *229*, 889. (c) Yamamoto, S.; Hayaishi, O. *J. Biol. Chem.* **1967**, *242*, 5260. (d) Yoshida, R.; Hayaishi, O. *Methods Enzymol.* **1987**, *142*, 188. (e) Sono, M.; Roach, M. P.; Coulter, E. D.; Dawson, J. H. *Chem. Rev.* **1996**, *96*, 2841.

(2) Nonenzymatic reactions of indole derivatives with O_2:(a) Philbrook, G. F.; Qyers, J. B.; Totter, J. R. *Photochem. Photobiol.* **1965**, *4*, 869. (b) Nishinaga, A. *Chem. Lett.* **1975**, 273. (c) Dufour-Ricroch, M. N.; Gaudemer, A. *Tetrahedron Lett.* **1976**, *17*, 4079. (d) Nakagawa, M.; Watanabe, H.; Kodato, S.; Okajima, H.; Hino, T.; Flippen, J. L.; Witkop, B. *Proc. Natl. Acad. Sci. U.S.A.* **1977**, *74*, 4730. (e) Saito, I.; Matsuura, T.; Nakagawa, M.; Hino, T. *Acc. Chem. Res.* **1977**, *10*, 346.

(3) Knox, W. E.; Mehler, A. H. *J. Biol. Chem.* **1950**, *187*, 419.

(4) Shimizu, T.; Nomiyama, S.; Hirata, F.; Hayaishi, O. *J. Biol. Chem.* **1978**, *253*, 4700.

(5) (a) Mellor, A. L.; Munn, D. H. *Nat. Rev. Immunol.* **2004**, *4*, 762. (b) Grohmann, U.; Fallarino, F.; Puccetti, P. *Trends Immunol.* **2003**, *24*, 242. (c) Uyttenhove, C.; Pilotte, L.; Theate, I.; Stroobant, V.; Colau, D.; Parmentier, N.; Boon, T.; van den Eynde, B. J. *Nat. Med.* **2003**, *9*, 1269. (d) Takikawa, O. *Biochem. Biophys. Res. Commun.* **2005**, *338*, 12. (e) Muller, A. J.; Scherle, P. A. *Nat. Rev. Cancer* **2006**, *6*, 613. (f) Katz, J. B.; Muller, A. J.; Prendergast, G. C. *Immunol. Rev.* **2008**, *222*, 206.

Scheme 1. Recently Proposed Pathways for IDO/TDO

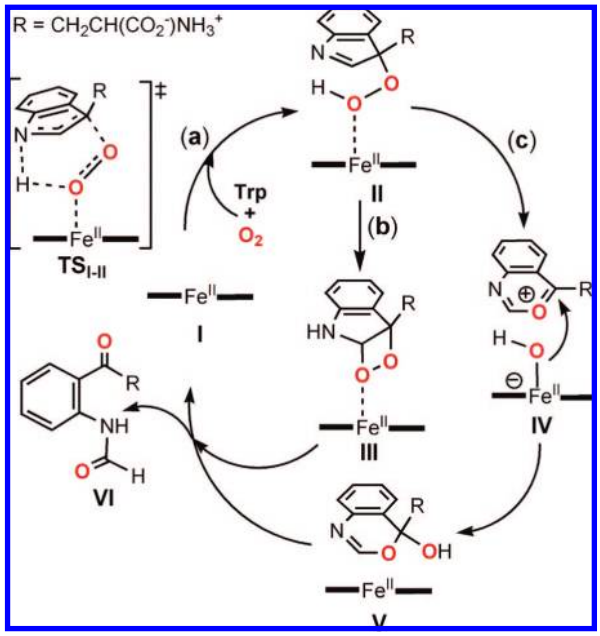

as due to the fact that no similar reaction is observed in the other heme-containing oxygenases.

Very recently, three groups independently obtained X-ray crystal structures of IDO and TDO[7] and advanced our understanding of a missing piece in heme chemistry. Structural analysis and site-directed mutagenesis studies showed that polar residues in the active site (Ser167, Cys129, and Ser263 of human IDO (hIDO), Tyr130 of *Ralstonia metallidurans* TDO (rmTDO), and His55 of *Xanthomonas campestris* TDO (xcTDO)) do not play an important role in the enzymatic reaction.[7] In addition, no hydrogen-bond network with bulk water solvent was observed in the distal pocket of the enzymes. Therefore, it seems that IDO and TDO do not require polar residues or water molecule for the enzymatic reactions; this is certainly different from the heme-containing monooxygenases or nonheme dioxygenases.[1e,6] Although a hydrogen-bond network with the proximal histidine was observed in hIDO and xcTDO crystal structures and some imidazolate characters of that histidine in human IDO and TDO were implied by recent resonance Raman spectroscopy studies,[7,8] the role of the imidazolate character (push effect) in the reaction remains unresolved. On the other hand, substitution of the indole NH group by one NMe group, oxygen, or sulfur atom renders the organic substrate to be a competitive inhibitor of IDO.[1e] It implicates the importance of the NH group in the enzymatic reaction. Moreover, an electron-donating group on the indole or electron-withdrawing group on the porphyrin enhances the reaction rate.[1e]

Scheme 2. Truncated Heme (**1**) and Trp (**i**) Models for IDO/TDO in our DFT Study

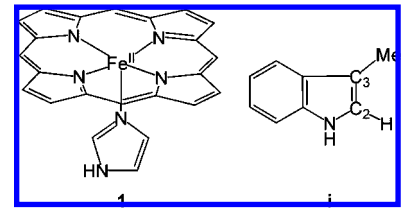

On the basis of these experimental observations, two new mechanistic pathways initiating with electrophilic addition of Fe(II)-bound dioxygen coupled with proton transfer (concerted oxygen ene-type reaction) via $\mathbf{TS_{I-II}}$ followed by either formation of a dioxetane intermediate **III** (route b) or Criegee-type rearrangement (route c) were accordingly proposed (Scheme 1).[7−9] The dioxetane formation pathway is controversial, partly because of ring strain. Instead, the Criegee-type rearrangement pathway, which occurs in the catechol dioxygenases,[6a,c,10] was suggested to be the dominant pathway for indole derivatives under nonenzymatic conditions.[11a,b] Overall, these proposed mechanisms are exceptional, because IDO and TDO do not require external proton, base, or electron reductant.[12*] Additionally, they catalyze oxidation with the same and low oxidation state of the iron(II) center (Scheme 1).

However, we suspected that the proposed concerted oxygen ene-type reaction via $\mathbf{TS_{I-II}}$ should be energetically unfavorable, because the N−H bond of the indole has to be bent significantly and, in turn, conjugation stabilization for the nitrogen lone pair must be lost. Although protonation on the nitrogen can lead to a better structure for the concerted oxygen ene-type transition state, a very strong acid is required and protonation would preferentially occur at the C3 position.[13] An alternative mechanistic pathway for the dioxygen activation in IDO and TDO should then be explored.

We performed density functional theory (DFT) calculations to elucidate the alternative reaction mechanism in IDO and TDO by using simplified enzymatic model complexes shown in Scheme 2.[14,15] As previously discussed, on the basis of the crystal structures and mutagenesis studies,[7] water molecule in the distal pocket was considered to be absent and several polar amino acids in the distal pocket do not have a strong effect on

(6) (a) Colas, C.; Ortiz de Montellano, P. R. *Chem. Rev.* **2003**, *103*, 2305. (b) Costas, M.; Mehn, M. P.; Jensen, M. P.; Que, L., Jr *Chem. Rev.* **2004**, *104*, 939. (c) Meunier, B.; de Visser, S. P.; Shaik, S. *Chem. Rev.* **2004**, *104*, 3947. (d) Abu-Omar, M. M.; Loaiza, A.; Hontzeas, N. *Chem. Rev.* **2005**, *105*, 2227. (e) Denisov, I. G.; Makris, T. M.; Sligar, S. G.; Schlichting, I. *Chem. Rev.* **2005**, *105*, 2253. (f) Shaik, S.; Kumar, D.; de Visser, S. P.; Altun, A.; Thiel, W. *Chem. Rev.* **2005**, *105*, 2279. (g) Poulos, T. L. *Biochem. Biophys. Res. Commun.* **2005**, *338*, 337. (h) *Ubiquitous Roles of Cytochrome P450 Proteins*; Sigel, A., Sigel, H., Sigel, R. K. O., Eds.; Metal Ions in Life Science; John Wiley & Sons Ltd.: West Sussex, U.K., 2007; Vol. 3.

(7) (a) Sugimoto, H.; Oda, S.-I.; Otsuki, T.; Hino, T.; Yoshida, T.; Shiro, Y. *Proc. Natl. Acad. Sci. U.S.A.* **2006**, *103*, 2611. (b) Forouhar, E.; Anderson, J. L. R.; Mowat, C. G.; Vorobiev, S. M.; Hussain, A.; Abashidze, M.; Bruckmann, C.; Thackray, S. J.; Seetharaman, J.; Tucker, T.; Xiao, R.; Ma, L.-C.; Zhao, L.; Acton, T. M.; Montelione, G. T.; Chapman, S. K.; Tong, L. *Proc. Natl. Acad. Sci. U.S.A.* **2007**, *104*, 473. (c) Zhang, Y.; Kang, S. A.; Mukherjee, T.; Bale, S.; Crane, B. R.; Begley, T. P.; Ealick, S. E. *Biochemistry* **2007**, *46*, 145.

(8) (a) Terentis, A. C.; Thomas, S. R.; Takikawa, O.; Littlejohn, T. K.; Truscott, R. J. W.; Armstrong, R. S.; Yeh, S.-R.; Stocker, R. *J. Biol. Chem.* **2002**, *277*, 15788. (b) Batabyal, D.; Yeh, S.-R. *J. Am. Chem. Soc.* **2007**, *129*, 15690.

(9) Prior to the electrophilic addition, deprotonation of Trp by the basic residue was proposed to proceed: (a) Hamilton, G. A. *Adv. Enzymol.* **1967**, *32*, 55 (cf. refs 1e and 8b).

(10) (a) Foster, T. L.; Caradonna, J. P. In *Comprehensive Coordination Chemistry II*; Que, L.; Tolman, W. B., Eds.; Elsevier: Oxford, 2004; Vol. 8, pp 343−368. (b) Borowski, T.; Siegbahn, P. E. M. *J. Am. Chem. Soc.* **2006**, *128*, 12941. (c) Borowski, T.; Georgiev, V.; Siegbahn, P. E. M. *J. Am. Chem. Soc.* **2005**, *127*, 17303. (d) Siegbahn, P. E. M.; Haeffner, F. *J. Am. Chem. Soc.* **2004**, *126*, 8919. (e) Bugg, T. D. H.; Lin, G. *Chem. Commun.* **2001**, 941.

(11) (a) Muto, S.; Bruice, T. C. *J. Am. Chem. Soc.* **1980**, *102*, 7379. (b) Witkop, B.; Patrick, J. B. *J. Am. Chem. Soc.* **1951**, *73*, 2196. (c) Fraser, M. S.; Hamilton, G. A. *J. Am. Chem. Soc.* **1982**, *104*, 4204.

(12) Electron transfer is needed to convert the inactive ferric state into the active ferrous form (ref 1e).

(13) Andonovski, B. S. *Croat. Chem. Acta* **1999**, *72*, 711.

the reactivity. Therefore, that simplified model should qualitatively mimic the enzymatic steps starting from the enzyme−substrate (oxyporphyrin−indole) complex **2**. The mechanism for the formation of the enzyme−substrate complex[1d,e] is not considered in these calculations. The outline of this paper is as follows. Computational methods are discussed in section 2. In section 3, Results and Discussion, feasibility of different pathways for the dioxygen activation process will be discussed first using a model in the absence and presence of porphyrin. Several possible pathways for the formation of formamido−ketone product in the presence of porphyrin are then examined. Effects of ionization of the imidazole and negatively charged oxyporphyrin complex on the key dioxygen activation steps are presented in the final part of this paper.

2. Computational Methods

All calculations were carried out with the Gaussian 03 program.[16] All geometries of reactants, transition states (TS), and intermediates were fully optimized with the B3LYP method.[17] Basis set 6-31G* was used for H, C, N, and O atoms. Hay−Wadt's effective core potentials (ECP) and basis sets were adopted for the Fe atom.[18] This basis set is labeled as BS1. Due to the huge computational cost, these calculations were mainly conducted in triplet and closed-shell singlet states (denoted by superscripts 3 and 1, respectively). Open-shell singlet state (denoted by superscript oss) calculations were carried out on the selected key stationary points. Generally, energies and structures for the triplet state are similar to those for the open-shell singlet state, as the two spins are weakly coupled. Wave function stability check was performed at all stationary points of the porphyrin-containing systems. Harmonic vibration frequency calculations were performed to characterize local minima and transition states and derive zero-point energy (ZPE). Single-point calculations on the critical steps were also performed at the BP86/BS1 level[19] and the B3LYP method with larger basis sets (BS2, 6-311G* for H, C, N, and O atoms, and Stuttgart/Dresden ECP and basis sets augmented with f-polarization functions for Fe).[20] Optimization and frequency calculations on some important points in Supporting Information Figures S1 and S2 were further carried out at BP86, B3PW91, M1PW1K, and PBEPBE functionals with BS1 as well as with the G2(MP2) method.[21,22] All energies presented in the text are relative electronic energies (corrected with ZPE, in kcal/mol) at the B3LYP/BS1 level, unless otherwise noted, relative to the isolated reactants (^{1}**1**, **i**, and $^3O_2$).[23]

3. Results and Discussion

We first performed preliminary calculations to study the feasibility of different dioxygen activation in the absence of porphyrin (dioxygen−indole complex). The detailed results were collected in the Supporting Information. The key findings are summarized as follows:

(1) The proposed concerted oxygen ene-type reaction has a very high barrier (41.9 kcal/mol), due to the highly distorted transition state.
(2) Direct electrophilic addition and, particularly, direct radical addition at the C2 position are thermodynamically more favorable than the C3 position, due to more resonance stabilization.
(3) The dioxetane pathway should not be neglected, as the dioxetane intermediate is calculated to be metastable, whereas the proposed Criegee-type rearrangement from the neutral 3-(hydroperoxy)indolenine intermediate requires a very high barrier (49.7 kcal/mol).

These preliminary results cast a doubt on the proposed concerted oxygen ene-type as the first step and the Criegee-type rearrangement pathway from the neutral intermediate as the second step.

3.1. Deoxyporphyrin and Oxyporphyrin−Indole Complexes. Guided by the preliminary calculations for dioxygen−indole complexes (without porphyrin) given in the Supporting Information, we examine structures and reactions in the presence of porphyrin in this and following sections. Figure 1 depicts the calculated structures of model deoxyheme (**1**) and oxyheme−indole (**2**) complexes. B3LYP calculations show that the high-

(14) One of the referees commented that a gas-phase mechanism can have nothing to do with the actual enzymatic mechanism. However, it has been well-documented that many mechanistic insights were primarily drawn from the gas-phase calculations (ref 15) rather than QM/MM calculations, such as, for the case of the heme systems, rebound mechanism, two (or multi)-state reactivity, chameleon nature of Cpd I, the feasibility of Cpd 0 as the second oxidant, the stepwise route for heme degradation from Cpd 0 in HO and oxidants for sulfur oxidation (ref 6f):(a) Shaik, S.; Hirao, H.; Kumar, D. *Acc. Chem. Res.* **2007**, *40*, 532. (b) Li, C.; Zhang, L.; Zhang, C.; Hirao, H.; Wu, W.; Shaik, S. *Angew. Chem., Int. Ed.* **2007**, *46*, 8168. (c) Hirao, H.; Kumar, D.; Thiel, W.; Shaik, S. *J. Am. Chem. Soc.* **2005**, *127*, 13007. (d) Kumar, D.; de Visser, S. P.; Sharma, P. K.; Cohen, S.; Shaik, S. *J. Am. Chem. Soc.* **2004**, *126*, 1907. (e) Sharma, P. K.; Kevorkiants, R.; de Visser, S. P.; Kumar, D.; Shaik, S. *Angew. Chem., Int. Ed.* **2004**, *43*, 1149. (f) de Visser, S. P.; Shaik, S.; Sharma, P. K.; Kumar, D.; Thiel, W. *J. Am. Chem. Soc.* **2003**, *125*, 15779. (g) Sharma, P. K.; de Visser, S. P.; Shaik, S. *J. Am. Chem. Soc.* **2003**, *125*, 8698. (h) Ogliaro, F.; de Visser, S. P.; Cohen, S.; Sharma, P. K.; Shaik, S. *J. Am. Chem. Soc.* **2002**, *124*, 2806.

(15) Selected recent theoretical studies by using the active-site model:(a) Dudev, T.; Lim, C. *Acc. Chem. Res.* **2007**, *40*, 85. (b) Yoshizawa, K. *Acc. Chem. Res.* **2006**, *39*, 375. (c) Siegbahn, P. E. M.; Borowski, T. *Acc. Chem. Res.* **2006**, *39*, 729. (d) Noodleman, L.; Lovell, T.; Han, W.-G.; Li, J.; Himo, F. *Chem. Rev.* **2004**, *104*, 459. (e) Himo, F.; Siegbahn, P. E. M. *Chem. Rev.* **2003**, *103*, 2421. (f) Siegbahn, P. E. M.; Blomberg, M. R. A. *Chem. Rev.* **2000**, *100*, 421. (g) Sicking, W.; Korth, H.-G.; de Groot, H.; Sustmann, R. *J. Am. Chem. Soc.* **2008**, *130*, 7345. (h) Robinet, J. J.; Cho, K.-B.; Gauld, J. W. *J. Am. Chem. Soc.* **2008**, *130*, 3328. (i) Aluri, S.; de Visser, S. P. *J. Am. Chem. Soc.* **2007**, *129*, 14846. (j) Leopoldini, M.; Russo, N.; Toscano, M. *J. Am. Chem. Soc.* **2007**, *129*, 7776. (k) Amano, T.; Ochi, N.; Sato, H.; Sakaki, S. *J. Am. Chem. Soc.* **2007**, *129*, 8131. (l) Kumar, D.; Hirao, H.; Shaik, S.; Kozlowski, P. M. *J. Am. Chem. Soc.* **2006**, *128*, 16148. (m) Green, M. T. *J. Am. Chem. Soc.* **2006**, *128*, 1902. (n) Kozlowski, P. M.; Kamachi, T.; Toraya, T.; Yoshizawa, K. *Angew. Chem., Int. Ed.* **2007**, *46*, 980. (o) de Visser, S. P. *Angew. Chem., Int. Ed.* **2006**, *45*, 1790.

(16) Pople, J. A.; et al. *Gaussian 03*, revision C.02; Gaussian, Inc.: Wallingford, CT, 2004.

(17) (a) Becke, A. D. *J. Chem. Phys.* **1993**, *98*, 5648. (b) Lee, C.; Yang, W.; Parr, R. G. *Phys. Rev. B* **1988**, *37*, 785.

(18) Hay, P. J.; Wadt, W. R. *J. Chem. Phys.* **1985**, *82*, 299.

(19) (a) Becke, A. D. *Phys. Rev. A* **1988**, *38*, 3098. (b) Perdew, J. P. *Phys. Rev. B* **1986**, *33*, 8822.

(20) (a) Dolg, M.; Wedig, U.; Stoll, H.; Preuss, H. *J. Chem. Phys.* **1987**, *86*, 866. (b) Martin, J. M. L.; Sundermann, A. *J. Chem. Phys.* **2001**, *114*, 3408.

(21) (a) Perdew, J. P.; Wang, Y. *Phys. Rev. B* **1992**, *45*, 13244. (b) Lynch, B. J.; Fast, P. L.; Harris, M.; Truhlar, D. G. *J. Phys. Chem. A* **2000**, *104*, 4811. (c) Perdew, J. P.; Burke, K.; Ernzerhof, M. *Phys. Rev. Lett.* **1996**, *77*, 3865. (d) Perdew, J. P.; Burke, K.; Ernzerhof, M. *Phys. Rev. Lett.* **1997**, *78*, 1396. (e) Curtiss, L. A.; Raghavachari, K.; Pople, J. A. *J. Chem. Phys.* **1993**, *98*, 1293.

(22) (a) Lynch, B. J.; Truhlar, D. G. *J. Phys. Chem. A* **2001**, *105*, 2936. (b) Parthiban, S.; de Oliveira, G.; Martin, J. M. L. *J. Phys. Chem. A* **2001**, *105*, 895. (c) Maranzana, A.; Ghigo, G.; Tonachini, G. *Chem. Eur. J.* **2003**, *9*, 2616.

(23) One of the referees is concerned that entropy effect could be important in the reaction involving the ring formation/breaking. The relative free energies of the key structures were put in Supporting Information Table S1. It is known that the free energies are overestimated in the gas phase and the entropic effect is not important in the enzyme. $\Delta E(\mathrm{ZPE})^{\ddagger}$ and/or $\Delta H^{\ddagger}$ values were suggested to study enzymatic reactivity in all practical purposes (cf., ref 6f). Moreover, in order to have consistent energetic profiles throughout the manuscript and to compare the protein effect by our ongoing ONIOM calculations, electronic energy profiles are, thus, used in this study.

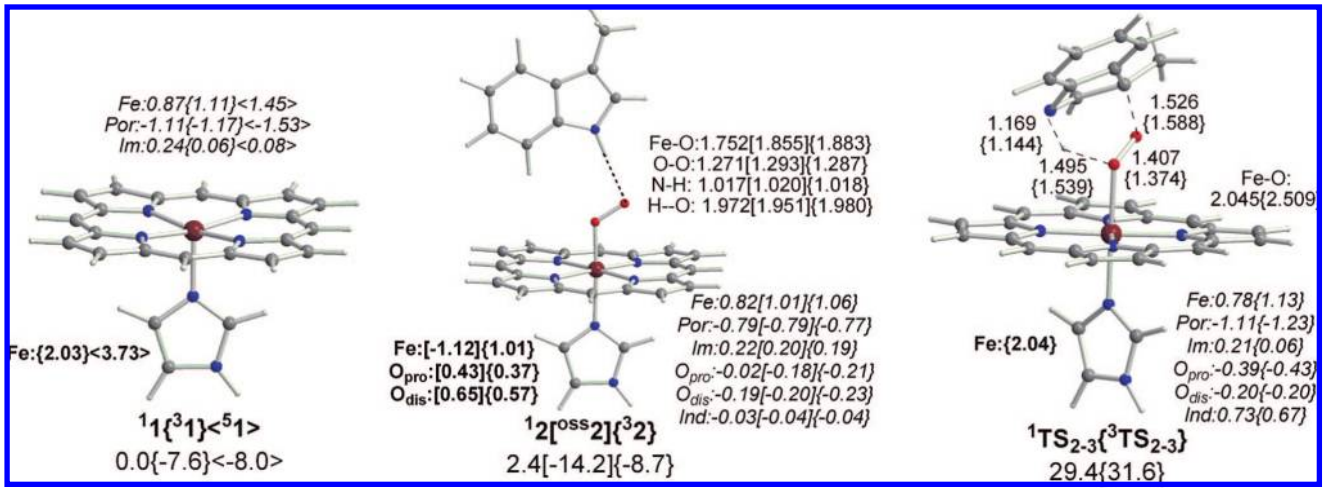

Figure 1. Calculated key structural parameters and relative energies (in kcal/mol) for model deoxyheme complexes (^{1,3,5}**1**), oxyheme−indole complexes (^{1,oss,3}**2**), and oxygen ene-type transition states (^{1,3}**TS$_{2-3}$**). Bond lengths (angstroms), natural charges, and Mulliken spin densities are in plain, italic, and bold fonts, respectively.

spin quintet state (^{5}**1**) is the most stable state of the deoxyporphyrin complex, whereas the low-spin open-shell singlet state (^{oss}**2**) is the most stable state of the oxyporphyrin−indole complex.[8a,24] On the basis of the Mulliken spin population, complexes ^{3}**2** and ^{oss}**2** can be regarded as ferric−superoxide complexes, in which one spin resides on Fe and the other one delocalizes over the dioxygen moiety. A larger amount of electron is transferred from the porphyrin to the dioxygen moiety in ^{oss,3}**2** (∼0.4 e) than ^{1}**2** (∼0.2 e). No stable oxyporphyrin−indole complex **2** in the quintet state can be located, as the dioxygen dissociates from the porphyrin. Therefore, the enzymatic reaction in a quintet state is not considered.

3.2. Dioxygen Activation. 3.2.1. Oxygen Ene-Type Pathway. The proposed electrophilic addition of O_2 to the indole in concert with proton transfer via ^{1,3}**TS$_{2-3}$** (oxygen ene-type reaction) is calculated to have a very high barrier (27.0−40.3 kcal/mol), with respect to the corresponding complexes ^{1,3}**2** (Figure 1). As discussed in our preliminary calculations in the Supporting Information, the N−H bond of the indole has to be bent significantly in these transition states. The reason for a higher barrier for the triplet state can be ascribed to a loss of an interaction between the proximal oxygen and Fe in ^{3}**TS$_{2-3}$**. In going from ^{3}**2** to ^{3}**TS$_{2-3}$**, the dioxygen and porphyrin moieties changed from doublet to singlet and from doublet to triplet, respectively. Consequently, the DFT calculations do not support the proposed concerted oxygen ene-type pathway responsible for the dioxygen activation in IDO and TDO.

3.2.2. Direct Electrophilic and Radical Addition Pathways. We now consider various direct additions of the bound dioxygen to the indole carbon *without the involvement of proton transfer* ("carbon-first" route) as alternative pathways. The relative position of L-Trp substrate in the distal pocket of xcTDO is schematically shown in Scheme 3.[7b] In principle, the dioxygen molecule can adopt two orientations (cis or trans) to attack two indole carbons (C2- or C3-addition pathway).[25] We are pleased

Scheme 3. Cis and Trans Addition Modes of Direct Addition

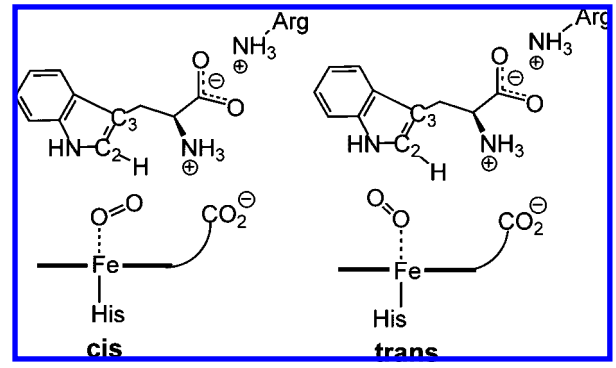

to show that the direct addition pathways have much lower barriers than the above-discussed concerted oxygen ene-type pathway, as shown in Figure 2 and Supporting Information Figures S5−S9. Our key findings of these alternative dioxygen activation pathways are summarized as follows.

(1) Changing orientation of the dioxygen (cis or trans) does not noticeably affect the reaction barriers, as seen between **TS$_{2-4a}$** and **TS$_{2-4b}$** and between **TS$_{2-4c}$** and **TS$_{2-4d}$**.

(2) In the case of the C3-addition pathways, the addition transition states have similar energies in different spin states, as seen in ^{1,oss,3}**TS$_{2-4a}$** as well as in ^{1,oss,3}**TS$_{2-4b}$**. On the other hand, in the C2-addition pathways, transition states in the triplet (or open-shell singlet) state (^{oss,3}**TS$_{2-4d}$**) are quite lower in energy than those in the closed-shell singlet state (^{1}**TS$_{2-4d}$**), apparently due to a larger stability of the addition products in the former states, as seen in ^{oss,3}**4$_d$** and ^{1}**4$_d$**. We failed to locate ^{1}**TS$_{2-4c}$**, due to very flat potential energy surface. The relative energy (without ZPE correction) of ^{1}**TS$_{2-4c}$** is estimated to be 15.4 kcal/mol, 1.0 kcal/mol higher than ^{1}**TS$_{2-4a}$** based on the relaxed scan calculations (Supporting Information Figure S7).

(3) Population analysis on the direct addition transition states and products in Figure 2 reveals that, in the closed-shell singlet state, the reaction takes place as electrophilic addition (with 2e transfer) to afford zwitterionic intermediates ^{1}**4a**−^{1}**4d** (∼0.7−0.9 e transferred from the indole to the oxyporphyrin). On the other hand, in the

(24) (a) Nakashima, H.; Hasegawa, J.-Y.; Nakatsuji, H. *J. Comput. Chem.* **2006**, *27*, 426. (b) Blomberg, L. M.; Blomberg, M. R. A.; Siegbahn, P. E. M. *J. Inorg. Biochem.* **2005**, *99*, 949.

(25) Prior to the availability of the X-ray crystal structure of xcTDO, two additional "conformers" were also considered (Supporting Information Figure S5). However, these two TSs are higher in energy and the indole in these two transition states fairly deviates from the X-ray crystal structure. Therefore, they are not considered in our study.

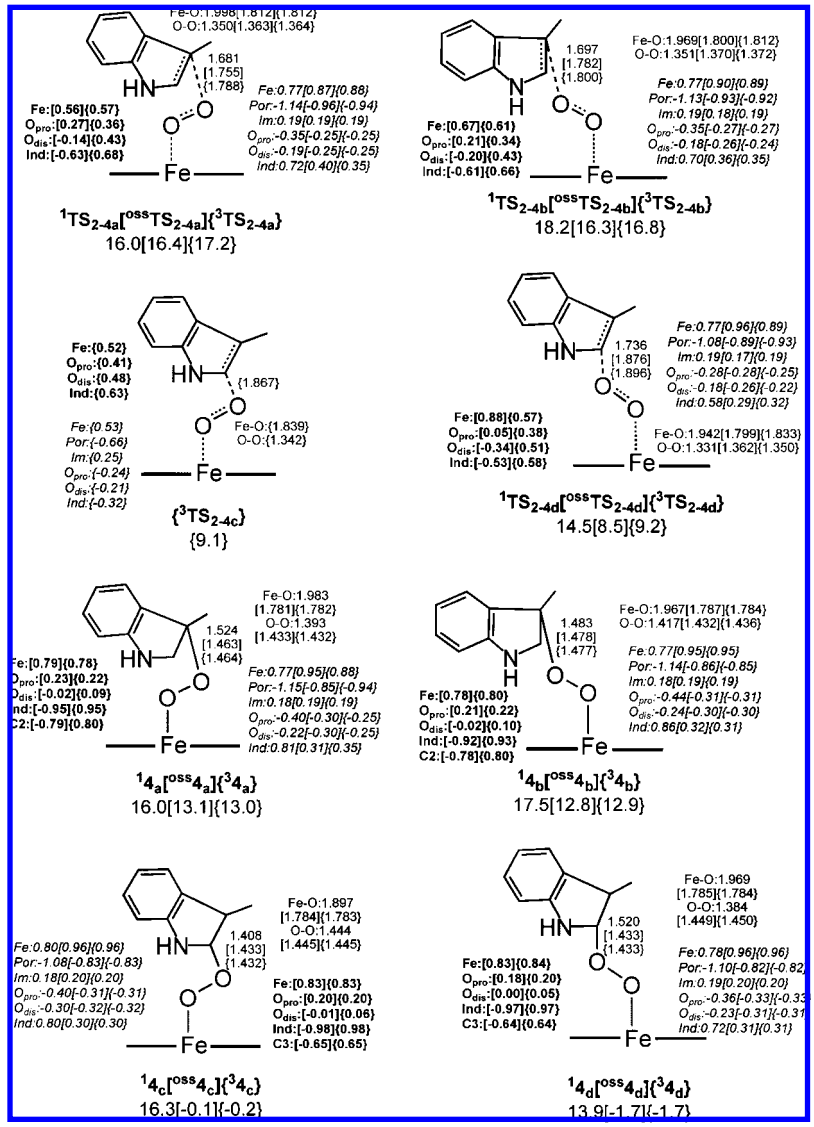

Figure 2. Calculated key structural parameters and relative energies (in kcal/mol) for direct electrophilic and radical addition transition states (**TS_{2-4a}**−**TS_{2-4d}**) and products (**4a**−**4d**). Bond lengths (angstroms), natural charges, and Mulliken spin densities are in plain, italic, and bold forms, respectively.

triplet (or open-shell singlet) state, the reaction takes place as radical addition (with 1e transfer) to give diradical ferric intermediates ^{oss,3}**4a**−^{oss,3}**4d** (∼0.3−0.4 e transferred).

(4) As shown in Figure 2, the most favorable TS for electrophilic addition is ^{1}**TS_{2-4d}** with a barrier of about 12.1 kcal/mol relative to ^{1}**2**, 23.2 kcal/mol relative to ^{3}**2**. For radical addition, the lowest-energy TS is ^{3}**TS_{2-4c}** and ^{3}**TS_{2-4d}** (17.8−17.9 kcal/mol relative to ^{3}**2**). Accordingly, the direct radical addition pathway that takes place in the triplet state is computed to be more favorable than the direct electrophilic addition pathway taking place in the singlet state, due to a higher stability of the resultant products.

(5) The indole plane is oriented fairly perpendicular to the porphyrin plane and the indole N−H bond points toward the porphyrin edge in many direct electrophilic and radical addition transition states (Supporting Information Figure S5). Particularly, the hydrogen and porphyrin carbons are in a close contact in some of these transition states, implying NH−π(porphyrin) interaction.[26] Such orientation could play an important role in hydrophobic interaction between Trp substrate and neighboring hydrophobic residues, because of the proposed strict shape complementarities between the substrate and protein side chain in the enzymatic reaction.[7a,b] However, quantum mechanics/molecular mechanics (QM/MM) calculations including the proteins are required to draw more quantitative conclusions. On the other hand, it is expected that methylation of Trp induces steric repulsion with the porphyrin edge in these direct addition transition states. Additionally, electron-poor benzo[*b*]furan and benzo[*b*]-thiophene analogs[27] should disfavor electron transfer and increase reaction barriers of the direct additions.[28]

3.2.3. Hydrogen Atom Transfer Pathway. In addition to the above direct electrophilic and radical addition pathways, both proton transfer and hydrogen atom transfer (i.e., proton-coupled

(26) One very strong NH−π interaction is found in ^{1}**TS_{2-4a}** and ^{1}**4a**. However, proton transfer to the porphyrin leading to ^{1}**4a′** is 3.5 kcal/mol less stable than ^{1}**4a** (Supporting Information Figure S8).

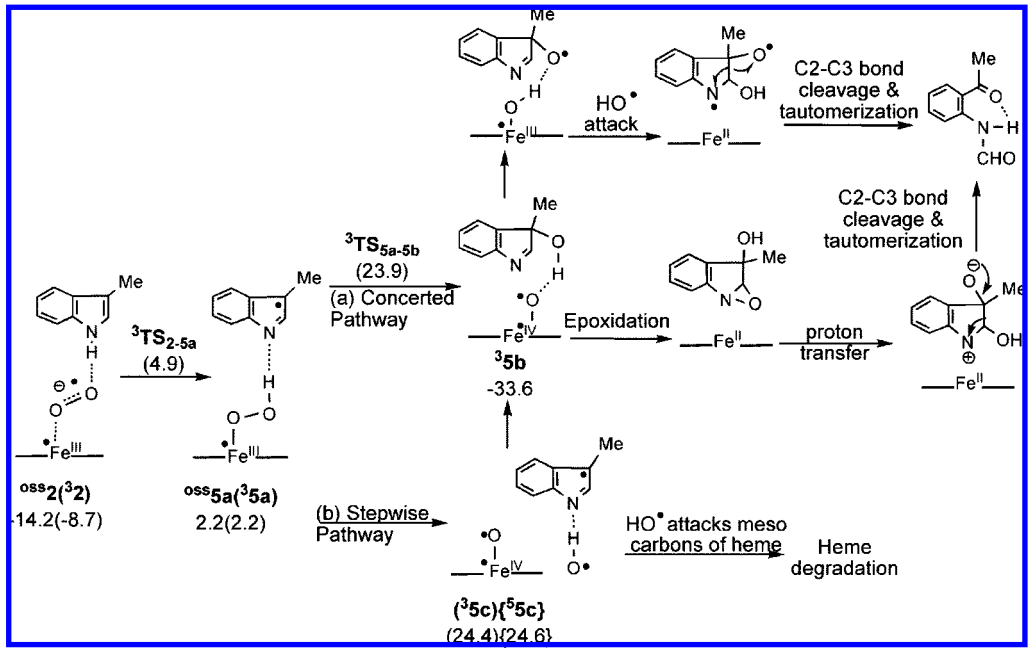

Figure 3. Relative energy profiles (in kcal/mol) of the hydrogen atom transfer pathway.

electron transfer) from the indole N−H bond to the distal oxygen of **2**, "hydrogen-first" routes, were studied, as shown in Figure 3. However, no proton-transfer transition state and product can be obtained in the closed-shell singlet surface, due to a very low acidity of the indole NH bond ($pK_a = 21$ in DMSO).[29] Hydrogen atom transfer transition state ^{3}**TS$_{2-5a}$** and product ^{3}**5a** can be located in the triplet state (Figure 3 and Supporting Information Figure S10). The barrier is 13.6 kcal/mol relative to ^{3}**2**, 4.2−4.3 kcal/mol lower in energy than the most favorable direct addition pathways. Analogous to heme oxygenase (HO),[1e,6a,30] ferric−hydroperoxy intermediate ^{3}**5a** could then react with the substrate (indole radical) in either a concerted or stepwise manner to give a hydroxylation product ^{3}**5b**. However, both the concerted pathway via ^{3}**TS$_{5a-5b}$** and the stepwise pathway via ^{3}**5c** are computed to be higher in energy than the direct addition pathways (Figures 2 and 3). Therefore, this HO-like pathway can not occur, but reversible hydrogen atom transfer from the indole nitrogen may proceed.

In summary, either the recently proposed concerted oxygen ene-type pathway or the hydrogen atom transfer pathway cannot be the first-step dioxygen activation process in IDO and TDO. Instead, we propose the new and favorable pathways for dioxygen activation in heme-containing IDO and TDO, which start with the direct radical (in the triplet state) or electrophilic (in the closed-shell singlet state) additions of the bound distal oxygen to the electron-rich indole carbon. In fact, the direct addition products **4a** and **4b** resemble the X-ray structure of Fe-bound indole−dioxygen adduct of nonheme naphthalene dioxygenase (NDO).[31] Therefore, our DFT calculations may further support a postulate that the direct radical or electrophilic addition of the Fe-bound dioxygen to alkenes or arenes for the formation of cis-diol derivatives may be another feasible mechanistic pathway.[32]

3.3. Formation of 2-Formamido-acetophenone Product. Now we examine the subsequent reaction pathways from the addition products **4a**−**4d**. Due to enormous computational cost to investigate all possibilities of several subsequent reaction pathways from all the addition products ^{1,3}**4a**−^{1,3}**4d**, intermediates ^{1,3}**4a** and ^{1,3}**4c** are mainly used as representatives in this part. The key results are summarized in Figure 4 Supporting Information Figures S11−S19.

3.3.1. Criegee-type Rearrangement Pathway. One-step Criegee-type rearrangement of 9-*trans*-decyl hydroperoxide benzoate and 11-hydroperoxytetrahydrocarbazolenine intermediates was proposed by Witkop and Bruice.[11a,b] This proposed one-step transition state requires that the $O_{pro}-O_{dis}$ bond is about anti to the C3−C2 bond. Intermediates ^{1,3}**4b** which fulfill such geometrical requirement were selected to study this one-step rearrangement. However, we could not locate the proposed one-step transition state accompanied by multiple bond-breaking and bond formation. Instead, the calculations led to very high energy transition states ^{1,3}**TS$_{4b}$**, as shown in Figure 4 and Supporting Information Figure S11.

Alternatively, prior to the Criegee-type rearrangement, intramolecular proton transfer or hydrogen atom transfer from the indole NH bond of intermediates **4** can occur to afford hydroperoxy intermediates, as shown in Figure 4 and Supporting Information Figure S12. However, the indole NH bond in the

(27) *N*-Methylindole is about 10 orders of magnitude more electrophilic than benzo[*b*]furan and benzo[*b*]thiophene: Mayr, H.; Kempf, B.; Ofial, A. R. *Acc. Chem. Res.* **2003**, *36*, 66.

(28) The preliminary calculations on the substrate effect were also carried out (Supporting Information Figure S9). *N*-Methylindole as the substrate has a higher relative energy for the direct electrophilic addition transition state (20.5 kcal/mol) but a similar energy for the direct radical addition transition state. No direct electrophilic addition transition state and product could be located, when electron-poorer benzo[*b*]furan was used. Also, benzo[*b*]furan slightly increases the relative energy of the direct radical addition to 11.3 kcal/mol. The substrate effect will be extensively studied in our QM/MM studies.

(29) Bordwell, F. G. *Acc. Chem. Res.* **1988**, *21*, 456.

(30) (a) Kumar, D.; de Visser, S. P.; Shaik, S. *J. Am. Chem. Soc.* **2005**, *127*, 8204. (b) Kamachi, T.; Yoshizawa, K. *J. Am. Chem. Soc.* **2005**, *127*, 10686.

(31) Carredano, E.; Karlsson, A.; Kauppi, B.; Choudhury, D.; Parales, R. E.; Parales, J. V.; Lee, K.; Gibson, D. T.; Eklund, H.; Ramaswamy, S. *J. Mol. Biol.* **2000**, *296*, 701.

(32) Bertini, I.; Briganti, F.; Scozzafava, A.; Luchinat, C. *New J. Chem.* **1996**, *20*, 187.

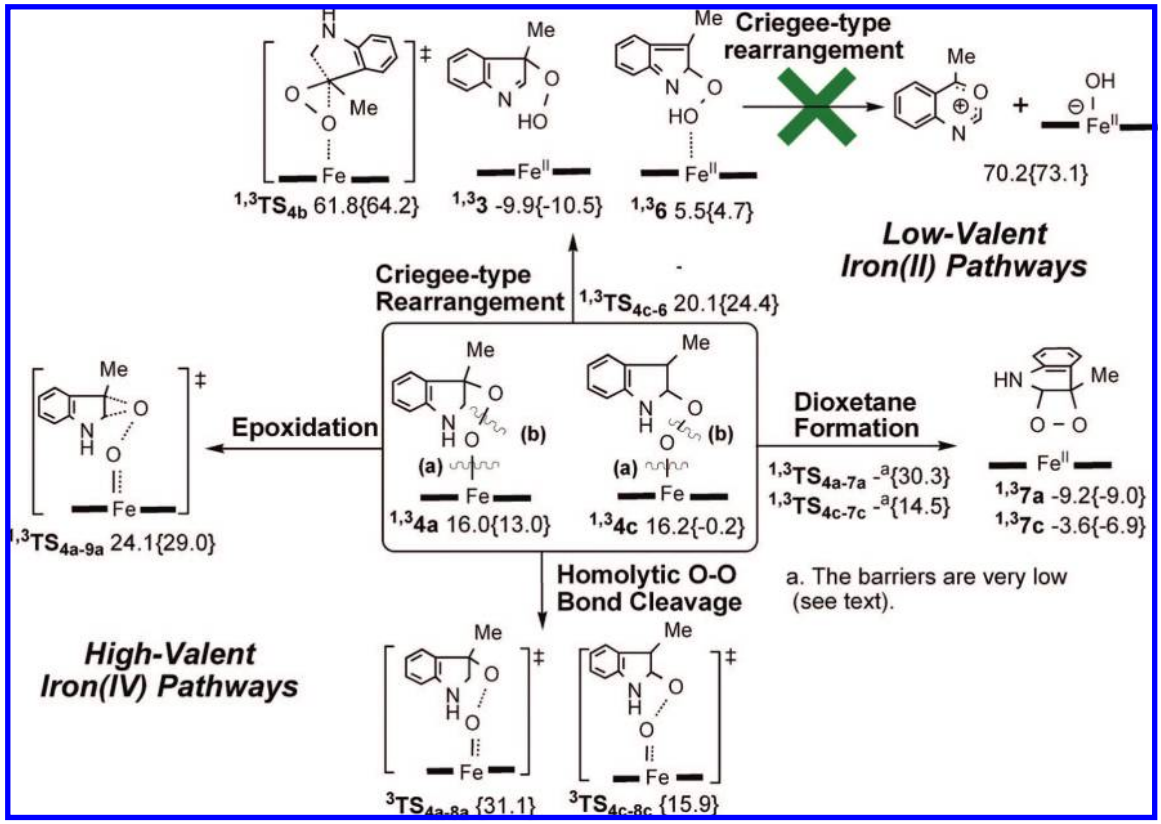

Figure 4. Energy profiles (in kcal/mol) for various pathways to give 2-formamido-acetophenone product.

"trans" intermediates, ^{1,3}**4b** and ^{1,3}**4d**, is far away from the proximal oxygen (Figure 3 and Supporting Information Figure S6). Significant rearrangement of the indoleine part is needed for such transformation, which is considered to be less possible. On the other hand, the "cis" intermediates ^{1,3}**4c**, which give ^{1,3}**TS$_{4c-6}$** (leading to ^{1,3}**6**), are quite high in energy (20.1−24.4 kcal/mol) as shown in Figure 4, because even here the N−H bond is needed to be distorted substantially in these transition states (Supporting Information Figure S12).[33] Many tries to locate the Criegee-type rearrangement transition state from ^{1,3}**3** and ^{1,3}**6** intermediates were unsuccessful, presumably due to the high-energy transition state for kinetically and thermodynamically unfavorable Criegee-type rearrangement from the neutral intermediates, as shown in the case without the porphyrin in Supporting Information Figures S2−S4. Instead, the calculations led to epoxide ring-opening transition states ^{1,3}**TS$_{S2-S3}$** (Supporting Information Figure S20). Consequently, the DFT calculations do not support the proposed Criegee-type rearrangement from the neutral intermediates of the present system. We may note that such rearrangement can proceed from the formally *anionic intermediates* in the catechol dioxygenases and other related nonheme oxygenases.[6,10] Since the Criegee-type rearrangement pathway is shown to be unlikely by the DFT calculations, two alternative routes involving cleavage of either Fe−O bond (route a in Figure 4) or O−O bond (route b) are then examined.

3.3.2. Dioxetane Pathway. We are pleased to find that the relative energy of ring-closure transition state ^{3}**TS$_{4c-7c}$** in the triplet state, which involves the Fe−O bond cleavage orchestrated with the C3−O$_{pro}$ bond formation to afford a dioxetane intermediate ^{3}**7c**, is calculated to be relative low (14.5 kcal/mol), 14.7 kcal/mol above ^{3}**4c**, as shown in Figure 4 and Supporting Information Figure S13. However, the relative energy of another ring closure via ^{3}**TS$_{4a-7a}$** is computed to be quite high (30.3 kcal/mol), lying 17.3 kcal/mol above the less stable intermediate ^{3}**4a**. More importantly, in the closed-shell singlet state, such ring-closure transition state cannot be located, but it is concluded to be nearly barrierless.[34] The relaxed scan calculations estimated a barrier of 1.8 kcal/mol to form ^{1}**7a** from ^{1}**4a** and nearly no barrier to afford ^{1}**7c** from ^{1}**4c** (Supporting Information Figures S14 and S15). Therefore, charge recombination easily proceeds from the zwitterionic intermediates. It should be noted that the formation of dioxetane intermediates ^{1,3}**7a** and ^{1}**7c** are slightly exothermic with respect to ^{1,3}**2**. Once the dioxetane is formed, it might leave the pocket and undergo ring-opening in the solution via ^{oss}**TS$_{iii-iv}$** (Supporting Information Figure S1). Alternatively, the heme metal center can act as a Lewis acid to catalyze ring-opening reaction. The first-step O−O bond cleavage of ^{1}**7a** involves spin-crossing with the triplet state and affords a diradical intermediate ^{3}**10a**, with a barrier of about 9.7 kcal/mol (without ZPE correction),[35] followed by essentially barrierless C2−C3 bond cleavage (Supporting Information Figure S17).[36] As a result, these DFT

(33) Unfortunately, several attempts to locate transition states from ^{1,3}**4a** to ^{1,3}**3** led to ^{1,3}**TS2−3**, in which the Fe−O$_{pro}$ and C3−O$_{dis}$ bonds were elongated. In fact, the transferring proton or hydrogen atom is far from the proximal oxygen in ^{1,3}**4a** (H−O$_{pro}$, 3.16−3.83 Å; N−H−O$_{pro}$, 53.4−57.6°; see Supporting Information Scheme S3), whereas less distortion from ^{1,3}**4c** is needed (H−O$_{pro}$, 2.90−2.94 Å; N−H−O$_{pro}$, 73.1−77.1°). Therefore, the reaction barriers for the intramolecular proton or hydrogen atom transfer from ^{1,3}**4a** should be higher than those starting from ^{1,3}**4c**.

(34) Attempts to locate intermediate ^{1}**4a2w** directly lead to the corresponding dioxetane intermediate, even starting from ^{3}**4a2w** (C2−O$_{pro}$, 2.850 Å, Supporting Information Figure S16).

Scheme 4. Route Involving Oxo Attack Followed by Facile C−C Bond Cleavage

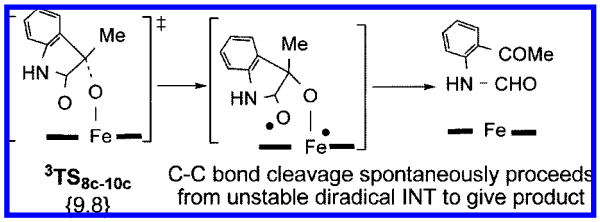

results suggest that, after the favorable direct triplet diradical or singlet electrophilic addition, the dioxetane formation pathway via radical or charge recombination seems to be a possible subsequent pathway in IDO and TDO.

3.3.3. Homolytic O−O Bond Cleavage Pathway. It is known that homolytic cleavage of the O−O bond can proceed from Fe(III)−alkylperoxo intermediates to give ferryl−oxo intermediates and alkoxy radicals.[6b,10b,c,37] ^{3}**TS$_{4c-8c}$** from the lower-energy intermediate ^{3}**4c** has a barrier of 16.1 kcal/mol and is lower in energy by 15.2 kcal/mol than ^{3}**TS$_{4a-8a}$** from the higher-energy intermediate ^{3}**4a**, as shown in Figure 4 and Supporting Information Figure S18. Once the O−O bond of ^{3}**4c** is homolytically broken, the most straightforward route leading to the product is oxo attack followed by barrierless C2−C3 bond cleavage (Scheme 4).[38] Since ^{3}**TS$_{4c-8c}$** is quite similar in energy to those for ^{1}**4a**, ^{1}**4c**, and ^{3}**TS$_{4c-7c}$**, the homolytic cleavage of the O−O bond and dioxetane formation pathways are suggested to operate concomitantly in the gas phase. However, effects of proteins, namely, electrostatic and steric interactions between the substrate and active-site residues, as well as stabilization preference toward the low- and high-valent iron center, might favor one of these pathways over the others. This will be the topic of our future QM/MM study. One may note, however, that the formation of the reactive ferryl−oxo intermediates might not be a desired pathway, because it might lead to the other unobserved side products.[39] Also, the formation of the highly electron-deficient ferryl−oxo intermediates might become less favorable, when the electron-withdrawing group is introduced to the porphyrin to promote the reaction rate.[1e]

3.3.4. Epoxidation Pathway. The last pathway we considered is homolytic cleavage of the O−O bond concerted with ring closure (i.e., epoxidation).[40] Interestingly, C−O bond is almost formed in epoxidation transition states ^{1,3}**TS$_{4a-9a}$** (1.52−1.54 Å), albeit the O−O bond is slightly elongated (1.61−1.69 Å, see Supporting Information Figure S19). Since ^{1,3}**TS$_{4a-9a}$** are calculated to be much higher in energy (24.1−29.0 kcal/mol) than the favorable homolytic cleavage of the O−O bond and dioxetane formation pathways (Figure 4), this epoxidation pathway should be less feasible.

Table 1. Calculated Relative Energies (in kcal/mol) of Key Intermediates and Transition States with Different Basis Sets and Different Functional, Corrected with ZPE at the B3LYP/BS1 Level

	B3LYP				B3LYP	
	BS1	BS2	BP86/BS1		BS1	BS2
^{1}**1**	0.0	0.0	0.0	^{3}**TS$_{4c-6}$**	24.4	24.2
^{5}**1**	−8.0	−12.7	12.1	^{3}**TS$_{4c-7c}$**	14.5	16.3
^{1}**2**	2.4	1.9	−21.4	^{1}**7a**	−9.2	−4.0
^{oss}**2**	−14.2	−16.3	−23.0	^{3}**7a**	−9.0	2.2
^{3}**2**	−8.7	−11.5	−19.9	^{1}**7c**	−3.6	2.3
^{1}**TS$_{2-3}$**	29.4	33.1	15.5	^{3}**7c**	−6.9	−0.4
^{3}**TS$_{2-3}$**	31.6	33.8	26.6	^{3}**TS$_{4a-8a}$**	31.1	30.0
^{1}**TS$_{2-4a}$**	16.0	18.5	0.3	^{3}**TS$_{4c-8c}$**	15.9	15.5
^{3}**TS$_{2-4c}$**	9.1	9.9	−5.4	^{1}**TS$_{4a-9a}$**	24.1	27.5
^{1}**4a**	16.0	18.6	1.8	^{3}**TS$_{4a-9a}$**	29.0	31.0
^{3}**4c**	−0.2	0.5	−10.0	^{1}**TS$_{8a-10a}$**	33.8	33.9
^{3}**TS$_{2-5a}$**	4.9	2.7	−12.1	^{3}**TS$_{8a-10a}$**	13.8	12.4
^{3}**TS$_{5a-5b}$**	23.9?	21.3	4.0	^{3}**TS$_{8c-10c}$**	9.8	7.9
^{3}**5c**	24.4	19.7	16.5	^{3}**10a**	−26.5	−26.3
^{1}**TS$_{4c-6}$**	20.1	22.9				

3.4. Effects of Basis Sets, Functionals, and Implicit Solvent. Energetic profiles obtained from the large basis set BS2 are generally similar to those calculated with the small basis set BS1. As shown in Table 1, the larger basis set BS2 also supports that the direct addition pathways are the most favorable pathway. Besides, the dioxetane pathway via ^{1}**4a**, ^{1}**4c**, and ^{3}**TS$_{4c-7c}$** are similar in energy to the homolytic O−O bond cleavage pathway via ^{3}**TS$_{4c-8c}$**. Therefore, the dioxetane and homolytic O−O bond cleavage pathways could compete with each other in the gas phase. Since B3LYP functional may overestimate stability of the high-spin species, the direct radical addition pathway may be biased. The BP86 functional was used to examine a few important stationary points (Table 1). The BP86 functional narrows energy difference between ^{3}**TS$_{2-4c}$** and ^{1}**TS$_{2-4a}$** to about 5.9 kcal/mol, but it overestimates the stability of the low-spin deoxyporphyrin complex ^{1}**1**. On the other hand, our proposed alternative pathways for dioxygen activation via ^{1}**TS$_{2-4a}$** and ^{3}**TS$_{2-4c}$** are still the most favorable ones by the BP86 method. Finally, one may imagine that the direct electrophilic addition (2e transfer) pathway in the singlet state may be stabilized by the protein environment more than the direct radical (1e transfer) pathway in the triplet state. We briefly performed single-point energy calculations by employing the polarizable continuum models (IEFPCM). We found that a continuum of uniform reaction field gives a similar solvation energy ($\Delta\Delta E_{solv} = 0.4$ kcal/mol) for both ^{1}**TS$_{2-4a}$** and ^{3}**TS$_{2-4c}$**.[41]

3.5. Effect of Ionization of the Imidazole and Negatively Charged Oxyporphyrin Complex. 3.5.1. The Anionic Imidazolate Ligand. X-ray crystallography and resonance Raman spectroscopy of human IDO showed that the proximal H346 is substantially ionized, facilitated by a hydrogen-bond network

(35) Minimum energy crossing point (MECP) is calculated to be about 9.7 kcal/mol above ^{1}**7a** (Supporting Information Figure S16). Minimum energy crossing point was located by Harvey's code: Harvey, J. N.; Aschi, M.; Schwarz, H.; Koch, W. *Theor. Chem. Acc.* **1998**, *99*, 95.

(36) The corresponding diradical intermediate derived from homolytic O−O bond cleavage of ^{3}**10c** cannot be located. The subsequent C−C bond cleavage proceeds directly and gives 2-formamido-acetophenone product.

(37) (a) Kojima, T.; Leising, R. A.; Yan, S.; Que, L., Jr *J. Am. Chem. Soc.* **1993**, *115*, 11328. (b) Kim, J.; Harrison, R. G.; Kim, C.; Que, L., Jr *J. Am. Chem. Soc.* **1996**, *118*, 4373. (c) Lehnert, N.; Ho, R. Y. N.; Que, L., Jr *J. Am. Chem. Soc.* **2001**, *123*, 8271. (d) Bassan, A.; Blomberg, M. R. A.; Siegbahn, P. E. M.; Que, L., Jr *J. Am. Chem. Soc.* **2002**, *124*, 11056. (e) Kryatov, S. V.; Rybak-Akimova, E. V.; Schindler, S. *Chem. Rev.* **2005**, *105*, 2175.

(38) Other pathways were also studied (Supporting Information Figures S18 and S20).

(39) Dehydrogenation of 3-methylindole to 3-methyleneindolenine by cytochrome P450: Skiles, G. L.; Yost, G. S. *Chem. Res. Toxicol.* **1996**, *9*, 291.

(40) IRC calculations confirmed that ^{1,3}**TS$_{4a-9a}$** can connect to ^{1,3}**4a**.

(41) Basis set 6-311++G** was used for H, C, N, and O atoms; Hay−Wadt's ECP and basis sets were used for Fe; ether ($\varepsilon = 4.335$) as the solvent and radii = UAKS and SCFVAC were adopted to estimate the solvation energy:(a) Cossi, M.; Scalmani, G.; Rega, N.; Barone, V. *J. Chem. Phys.* **2002**, *117*, 43. (b) Cancès, M. T.; Mennucci, B.; Tomasi, J. *J. Chem. Phys.* **1997**, *107*, 3032. (c) Cossi, M.; Barone, V.; Mennucci, B.; Tomasi, J. *Chem. Phys. Lett.* **1998**, *286*, 253. (d) Mennucci, B.; Tomasi, J. *J. Chem. Phys.* **1997**, *106*, 5151.

Table 2. Calculated Relative Energies (in kcal/mol) of the System with Anionic Imidazolate Ligand (**Imz**$^-$) and Negatively Charged Oxyporphyrin System (**e**$^-$), Compared with the Neutral System

	neutral	(**Imz**$^-$)	(**e**$^-$)[a]
^{1}**1**	0.0	0.0	0.0 (D)
^{5}**1**	−8.0	−12.6	
^{1}**2**	2.4	−7.1	−38.8 (D)
^{3}**2**	−8.7	−22.8	
^{1}**TS$_{2-4a}$**	16.0	*b*	12.0 (D)
^{3}**TS$_{2-4a}$**	17.2	15.9	19.3 (Q)
^{1}**TS$_{2-4c}$**	14.5	17.5	−5.3 (D)
^{3}**TS$_{2-4c}$**	9.1	5.0	8.8 (Q)

[a] The relative energy of the doublet (D) and quartet (Q) states is relative to the isolated reactants (^{1}**1**, **i**, and O_2^-). [b] The direct electrophilic addition transition states and corresponding stable products cannot be located.

Scheme 5. Geometrical Features of One Neutral and Two Anionic Oxyporphyrin−Indole Complexes

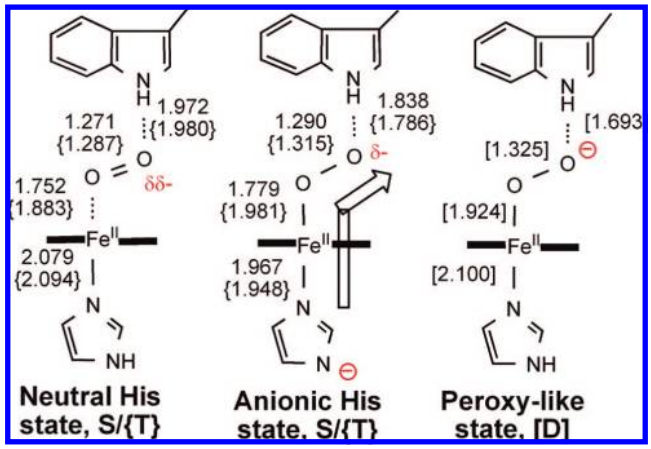

with two water molecules, L388 carbonyl oxygen, and heme 6-propionate.[7a,8] However, effects of the ionization of the proximal histidine on the reactivity remain unclear. Therefore, the neutral imidazole ligand is replaced by an anionic imidazolate ligand (appended by (**Imz**$^-$)) to examine the key dioxygen steps, as shown in Table 2 and Supporting Information Figure S21. The calculations show that stability of the oxyporphyrin−indole complexes ^{1,3}**2**(**Imz**$^-$) increases with the complete ionization, because the anionic ligand increases negative charge of the dioxygen moieties (push effect) and, thus, strengthens the hydrogen bond between the distal oxygen and indole, as shown in Scheme 5. However, we would expect that the direct electrophilic addition from the lesser electron-deficient complexes ^{1,3}**2**(**Imz**$^-$) to the electron-rich indole should become less favorable. In fact, no electrophilic addition product ^{1}**4a**(**Imz**$^-$) and transition state ^{1}**TS$_{2-4a}$**(**Imz**$^-$) can be obtained from our calculations, as the C3−O_{dis} bond is completely broken. The direct electrophilic addition via ^{1}**TS$_{2-4c}$**(**Imz**$^-$) lies 40.3 kcal/mol above ^{3}**2**(**Imz**$^-$). The anionic imidazole ligand also raises the barrier for the direct radical addition via ^{3}**TS$_{2-4a}$**(**Imz**$^-$) and ^{3}**TS$_{2-4c}$**(**Imz**$^-$) to 38.7 and 27.8 kcal/mol, respectively. The other dioxygen activation processes are also computed to be unfavorable with the anionic imidazolate ligand. ^{1}**TS$_{2-3}$**(**Imz**$^-$) and ^{3}**5c**(**Imz**$^-$) are higher in energy than ^{3}**2**(**Imz**$^-$) by 59.6 and 44.5 kcal/mol, respectively. Higher reaction barriers should be partly attributed to a loss of a stronger hydrogen bond in these addition transition states, relative to the enzyme−substrate complexes. Therefore, the reaction barrier would be overestimated if Trp does not form a hydrogen bond with the bound dioxygen. However, the recent resonance Raman spectroscopy studies implied strong hydrogen bonding in hIDO, but not in hTDO.[8] As to the dioxygen activation process, it should be noted that reaction with *electrophilic substrates* in peroxidase and the other heme oxygenases, which can be promoted by electron donation from the proximal ligand to the metal (push effect), is completely different from reaction with the *nucleophile*, Trp, in IDO or TDO. It is in line with experimental observations that electron-withdrawing group on the porphyrin increases enzymatic rate.[1e] The above DFT calculations show that complete or substantial ionization of the proximal histidine should play a detrimental role in the first-step addition with Trp. Therefore, we propose that IDO could finely tune the degree of the ionization of the proximal histidine for complexation and electrophilic addition.

3.5.2. Negatively Charged Oxyporphyrin Complex. Since electron transfer occurs in the dioxygen activation process of some heme-containing enzymes (e.g., P450, see Scheme 6), and superoxide anion can be uniquely used as the oxygen source for the inactive form of IDO,[42] one extra electron is added to the neutral complex **2** to mimic effects of electron transfer or superoxide anion for the active ferrous form of IDO (appended by (**e**$^-$)). Similar to the case with the anionic imidazolate ligand, a very stable anionic oxyporphyrin−indole complex ^{2}**2**(**e**$^-$) is formed with a very strong hydrogen bond (H−O, 1.69 Å) in the doublet state, as shown in Scheme 5 and Supporting Information Figure S22. The computed O−O bond is also elongated to 1.33 Å in ^{2}**2**(**e**$^-$) (more peroxy character). However, the reaction barriers of the direct additions via ^{2}**TS$_{2-4a}$**(**e**$^-$), ^{4}**TS$_{2-4a}$**(**e**$^-$), ^{2}**TS$_{2-4c}$**(**e**$^-$), and ^{4}**TS$_{2-4c}$**(**e**$^-$) increase to 50.8, 58.1, 33.5, and 47.6 kcal/mol, respectively, relative to the very stable complex ^{2}**2**(**e**$^-$) (Table 2). Consequently, the DFT calculations do not favor extra electron transfer or superoxide anion as the oxygen source for the reduced ferrous form of IDO, because the very strong hydrogen bond is broken during the addition and electrophilicity of the bound dioxygen is decreased in the negatively charged oxyporphyrin−indole complex ^{2}**2**(**e**$^-$). Scheme 6 illustrates the generally accepted active species and oxidation mechanisms of various heme systems, in which we note that

Scheme 6. Dioxygen Activation Process for IDO/TDO and Other Heme Systems

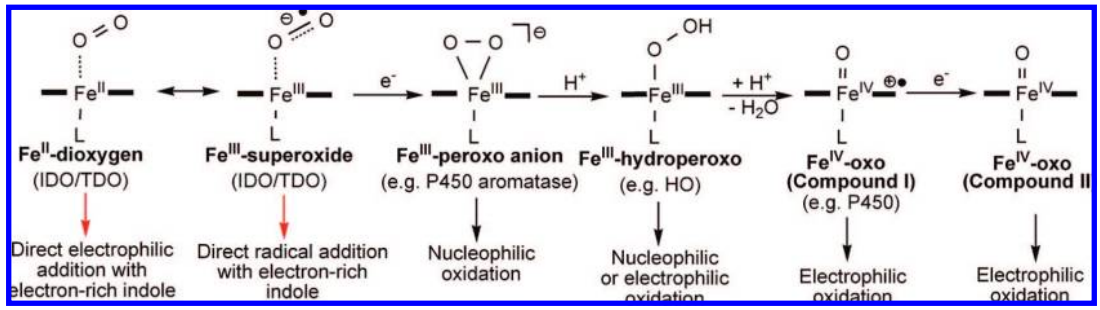

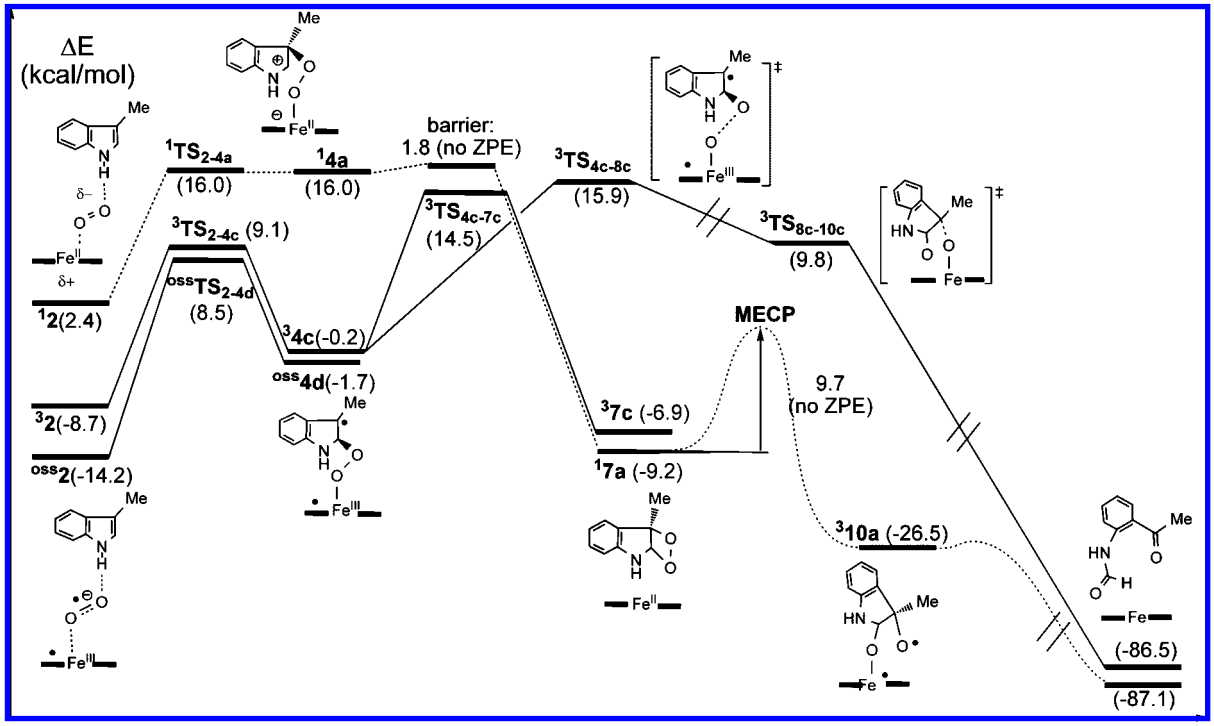

Figure 5. Potential energy surface for the proposed new mechanistic pathway for IDO and TDO.

Scheme 7. Proposed New Mechanism for IDO and TDO

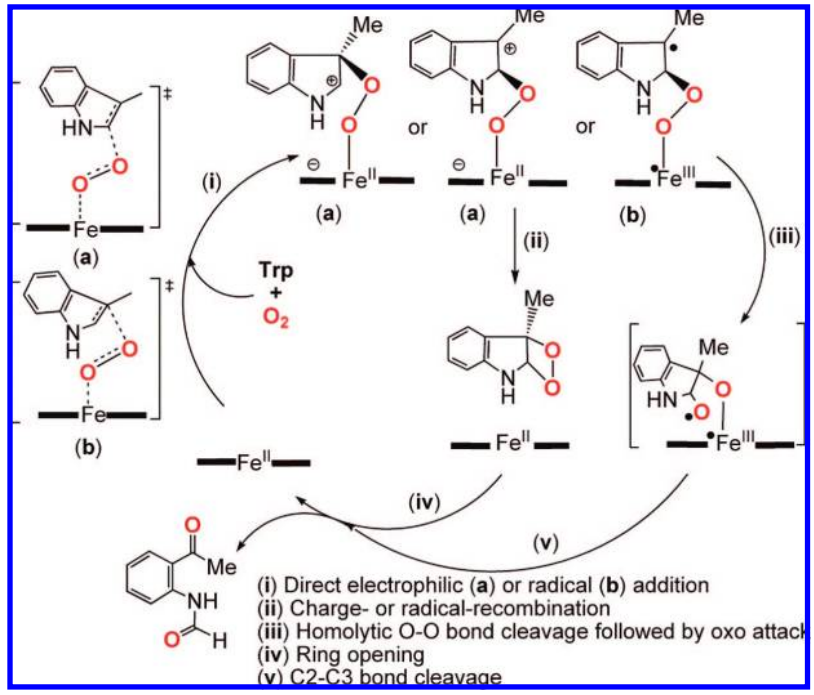

ferric−peroxo anion porphyrin complexes were reported to undergo nucleophilic reaction with electron-poor substrates.[43,44]

4. Conclusions

DFT calculations have been performed to elucidate the new reaction mechanism of oxidative cleavage of Trp in IDO and TDO. As shown in Figure 5 and Scheme 7,[45] the key findings of our study are summarized as follows.

(1) For the dioxygen activation step, the proposed electrophilic addition concerted with proton transfer (i.e., concerted oxygen ene-type reaction) has a very high barrier because of highly distorted transition state. Instead, a new and energetically favorable mechanistic pathway is proposed. It involves direct electrophilic (2e transfer pathway) or radical (1e transfer pathway) addition of the bound distal oxygen to the electron-rich indole carbon. Addition of C2 and C3 positions of the indole are computed to be feasible.

Our proposed new mechanism of dioxygen activation for these two unique heme-containing dioxygenases is

sharply distinct from the available mechanisms for the heme-containing oxygenases (Schemes 6 and 7).[1e,6,10,46,47] In IDO/TDO, the mild oxidant Fe(II)-bound dioxygen or Fe(III)−superoxide intermediate reacts with very electron-rich indole, whereas an extraordinarily strong oxidant ferryl−oxo intermediate (compound I) reacts with many unreactive substrates in P450 or peroxidase. It should be noted that the highly hydrophobic active-site pocket, the absence/no participation of the polar residues in the reaction, and the absence of a hydrogen-bond network with bulky water in the distal pocket of IDO and TDO should be important to protect the active and transient oxygenated species (e.g., **2** and **4**) for transferring both oxygen atoms to the substrate.[7a,b]

(2) The Criegee-type rearrangement pathway, which was proposed for the subsequent formation of *N*-formylkynurenine product, demands a very high barrier from the neutral indoleine intermediate. Instead, the zwitterionic and diradical products generated from the direct addition pathways undergo charge and radical recombination, respectively, to afford the comparatively stable dioxetane intermediates. Finally, metal-catalyzed ring-opening of the dioxetane intermediates easily takes place to give the product. Alternatively, the dioxetane formation pathway could compete with homolytic O−O bond cleavage followed by oxo attack and facile C2−C3 bond cleavage in the triplet surface. However, the formation of strong oxidant ferryl−oxo species in the latter pathway might lead to the undesired products.[39]

(3) (a) Complete ionization of the imidazole of the proximal histidine, (b) electron transfer to the active-form enzyme−substrate complex, and (c) superoxide anion as the oxygen source for the active ferrous form are found to significantly raise the reaction barrier for the dioxygen activation process, due to a loss of a strong hydrogen bond in the transition states and the decreased electrophilicity of the bound dioxygen intermediates.

The current DFT study sheds light on the reaction mechanisms for IDO and TDO at the atomic scale and further advances our understanding of the missing piece in heme chemistry. Different protein effects between IDO and TDO on the reaction mechanisms would be further understood by the experimental and our subsequent QM/MM studies.

Acknowledgment. We thank Drs. Marcus Lundberg and Ahmet Altun for useful discussions and suggestions. L.W.C. acknowledges the Fukui Institute Fellowship. This work is in part supported by the Japan Science and Technology Agency (JST) with a Core Research for Evolutional Science and Technology (CREST) Grant in the Area of High Performance Computing for Multiscale and Multiphysics Phenomena. The computational resource at Research Center of Computer Science (RCCS) at the Institute for Molecular Science (IMS) is also acknowledged.

Supporting Information Available: Complete ref 16, the calculated structures for the other intermediates and transition states, Cartesian coordinates, and absolute energies. This material is available free of charge via the Internet at http://pubs.acs.org.

JA803107W

(42) (a) Kobayashi, K.; Hayashi, K.; Sono, M. *J. Biol. Chem.* **1989**, *264*, 15280. (b) Hirata, F.; Ohnishi, T.; Hayaishi, O. *J. Biol. Chem.* **1977**, *252*, 4637.

(43) Wertz, D. L.; Valentine, J. S. In *Structure and Bonding*; Meunier, B.; Ed.; Springer-Verlag: Berlin, 2000; Vol. 97, pp 37−60.

(44) (a) Akhtar, M.; Lee-Robichaud, P.; Akhtar, M. E.; Wringh, J. N. *J. Steroid. Biochem. Mol. Biol.* **1997**, *61*, 127. (b) Vaz, A. D. N.; McGinnity, D. F.; Coon, M. J. *Proc. Natl. Acad. Sci. U.S.A.* **1998**, *95*, 3555. (c) Cryle, M. J.; De Voss, J. J. *Angew. Chem., Int. Ed.* **2006**, *45*, 8221.

(45) Due to the huge computational cost and similar electronic structures and energies to that triplet state in the key steps, the open-shell singlet state calculations were not extensively investigated. However, the reaction should also start from ^{oss}**2**, followed by similar pathways as the triplet state follows.

(46) Newcomb, M.; Shen, R.; Choi, S.-Y.; Toy, P. H.; Hollenberg, P. F.; Vaz, A. D. N.; Coon, M. J. *J. Am. Chem. Soc.* **2000**, *122*, 2677.

(47) During the manuscript preparation, electron transfer from carotenoid to non-heme iron-bound dioxygen complex and direct addition of the bound dioxygen following by either dioxetane or epoxidation formation pathway was proposed for oxidative cleavage of the C=C bond: Borowski, T.; Blomberg, M. R. A.; Siegbahn, P. E. M. *Chem. Eur. J.* **2008**, *14*, 2264.